

Evolution of the Insertion-Deletion Mutation Rate Across the Tree of Life

Way Sung,^{*,1,2} Matthew S. Ackerman,^{†,1} Marcus M. Dillon,^{*} Thomas G. Platt,^{†,**} Clay Fuqua,[†]

Vaughn S. Cooper,^{*,**} and Michael Lynch[†]

^{*}Department of Bioinformatics and Genomics, University of North Carolina at Charlotte, North Carolina 28223,

[†]Department of Biology, Indiana University, Bloomington, Indiana 47405, [‡]Microbiology Graduate Program, University of New Hampshire, Durham, New Hampshire 03824, [§]Division of Biology, Kansas State University, Manhattan, Kansas 66506, and ^{**}Department of Microbiology and Molecular Genetics, University of Pittsburgh School of Medicine,

Pennsylvania 15219

ORCID ID: 0000-0002-8336-8913 (W.S.)

ABSTRACT Mutations are the ultimate source of variation used for evolutionary adaptation, while also being predominantly deleterious and a source of genetic disorders. Understanding the rate of insertion-deletion mutations (indels) is essential to understanding evolutionary processes, especially in coding regions, where such mutations can disrupt production of essential proteins. Using direct estimates of indel rates from 14 phylogenetically diverse eukaryotic and bacterial species, along with measures of standing variation in such species, we obtain results that imply an inverse relationship of mutation rate and effective population size. These results, which corroborate earlier observations on the base-substitution mutation rate, appear most compatible with the hypothesis that natural selection reduces mutation rates per effective genome to the point at which the power of random genetic drift (approximated by the inverse of effective population size) becomes overwhelming. Given the substantial differences in DNA metabolism pathways that give rise to these two types of mutations, this consistency of results raises the possibility that refinement of other molecular and cellular traits may be inversely related to species-specific levels of random genetic drift.

KEYWORDS

insertion-deletion
mutation rate
mutation-rate
evolution
drift barrier
mutation
accumulation

Mutations are a double-edged sword in all organisms, constituting the ultimate source of variation used for evolutionary adaptation, while also being predominantly deleterious and a source of genetic disorders. Hence, researchers have long sought the primary factors governing mutation-rate evolution. Some have argued that the mutation rate of an organism reflects a balance between the deleterious effect of mutations and physiological limitations, with further refinement of replication fidelity limiting the speed of DNA synthesis

necessary for efficient daughter-cell production (Drake 1991; Sniegowski *et al.* 2000). However, replication fidelity can be improved without a significant decrease in doubling time (Loh *et al.* 2010), and prokaryotes undergo high cell-division rates and have low mutation rates (Drake 1991; Lynch 2010), suggesting that replication fidelity does not limit the rate of daughter-cell production. Furthermore, because there is no negative correlation between cell-division rate and genome size (Mira *et al.* 2001; Vieira-Silva *et al.* 2010), and the reverse may even be true in bacteria (Lynch and Marinov 2015), cell-division rates do not appear to be limited by the amount of DNA synthesized. Thus, alternative forces may govern mutation-rate evolution.

A general relationship describing mutation-rate variation was proposed by Drake *et al.* (1998), who suggested that the mutation rate per nucleotide site scales inversely with genome size in bacteria and unicellular eukaryotes, such that there is a constant ~ 0.003 mutations per haploid genome per cell division. However, as direct estimates of mutation rates for additional organisms became available, the general relationship between genome size and mutation rate became less apparent, even when scaled to the number of cell divisions per generation in multicellular species (Lynch 2010).

Copyright © 2016 Sung *et al.*

doi: 10.1534/g3.116.030890

Manuscript received May 8, 2016; accepted for publication June 13, 2016; published Early Online June 15, 2016.

This is an open-access article distributed under the terms of the Creative Commons Attribution 4.0 International License (<http://creativecommons.org/licenses/by/4.0/>), which permits unrestricted use, distribution, and reproduction in any medium, provided the original work is properly cited.

Supplemental material is available online at www.g3journal.org/lookup/suppl/doi:10.1534/g3.116.030890/-/DC1

¹These authors contributed equally to this work.

²Corresponding author: Department of Bioinformatics and Genomics, University of North Carolina at Charlotte, 9201 University City Blvd. Charlotte, NC 28223.

E-mail: waysung@indiana.edu

In a previous analysis, we found a relationship between the base-substitution mutation rate per site per generation (u_{bs}) multiplied by the amount of functional DNA in a genome (G_e , approximated by proteome size), and the power of random genetic drift, which is inversely proportional to the effective population size (N_e) (Sung *et al.* 2012a). Because mutations are generally deleterious, this finding suggested that selection operates to reduce genome-wide mutation rates by refining DNA replication fidelity and repair until further improvements are too inconsequential to overcome the power of random genetic drift (Sniegowski and Raynes 2013). This result is consistent with the drift-barrier hypothesis (DBH), which proposes that natural selection operates to improve molecular and cellular traits until the selective advantage of a beneficial mutation refining the trait is so miniscule that the probability of it being fixed is essentially the same as that for neutral mutations (Lynch 2011; Sung *et al.* 2012a).

While the negative correlation between $u_{bs}G_e$ and N_e is consistent with expectations from population-genetic theory, there is a potential issue of circularity when correlating these factors, as the estimation of N_e relies indirectly on the estimation of u_{bs} (Sung *et al.* 2012a). Although we presented an analysis suggesting that the correlated parameters are not likely to be the primary factor in the observed relationship (Sung *et al.* 2012a), and provide another one here (Supplemental Material, File S1), a more independent analysis is desirable, and, given the amount of data that has accumulated, it is time to go beyond a study that simply considers base-substitution mutations. Here, we present the rate of insertion-deletion mutation (indel) events (u_{id}) per site per generation across eight eukaryotic and seven bacterial species, while also providing genome-wide estimates of u_{bs} and u_{id} from three new bacterial mutation-accumulation studies. These data continue to support a negative correlation between the genome-wide mutation rate and N_e .

The DBH postulates that genetic drift determines the limit of adaptive molecular refinement that can be achieved for any trait, including those that determine the rate of indels. Indels are a class of mutations separate from base substitutions, differing in how they originate. Indels generally arise from strand slippage or double-strand breaks, whereas base-substitution mutations originate primarily from base misincorporation or biochemical alteration. Furthermore, there are major differences in how the two mutation types are repaired. Base-substitution mutations are often reversed by enzymes such as DNA photolyases and alkyl transferases, which do not require DNA incision and synthesis (Sancar *et al.* 2004), or are identified by glycosylases in base-excision repair (BER) pathways, and repaired by incision and DNA-gap filling (Krokan and Bjoras 2013). On the other hand, indel mutations are not surveyed by BER, but are repaired primarily by nucleotide-excision repair (NER), which has broad substrate specificity, and is used to excise bulky lesions arising from the insertion or deletion of nucleotides (Morita *et al.* 2010). Although the mismatch-repair (MMR) pathway can operate on both base-substitution mutations and indels, MMR-deficient strains of *Escherichia coli* and *Caenorhabditis elegans* exhibit a significantly greater elevation of the indel mutation rate relative to that for base substitutions, providing further evidence for the differential treatment of mutation types by DNA-repair pathways (Denver *et al.* 2005; Lee *et al.* 2012). Furthermore, depending on the type of mismatch and local sequence context, the error rates of different polymerases are highly variable between indel and base-substitution mutations (McCulloch and Kunkel 2008; Kunkel 2009; Sung *et al.* 2015). In summary, because the enzymes influencing base-substitution and indel mutation rates differ (and shared enzymes differ in the spectrum of repaired pre-mutations), a focus on the indel mutation

rate provides a means of testing the validity of the DBH that is substantially independent biologically (and essentially fully independent in terms of investigator sampling) of that used to extrapolate measures of the power of random genetic drift.

Selection operates to refine DNA replication fidelity and repair when the genome-wide deleterious load confers a discernable fitness disadvantage on an organism (Kimura 1967, 1983; Lynch 2010), and the contributions of indel and base substitution mutations to genome-wide deleterious load differ in two ways. First, the effects of base substitutions in coding regions are highly variable (Eyre-Walker and Keightley 2007), and some base substitutions may not have any effect on organismal fitness, which may create some uncertainties in quantifying the effective genome size (G_e), thereby reducing the correlation observed between $u_{bs}G_e$ and N_e (Sung *et al.* 2012a). On the other hand, most indel mutations that arise in protein-coding genes will generate a frame-shift mutation, interfering with gene function, and having a direct effect on organismal fitness. Because such indels are generally deleterious, selection is then expected to more efficiently fine tune the rate at which indels arise, and, if the DBH holds true, this should yield a close correlation between $u_{id}G_e$ and N_e . Second, base-substitutions are generally limited to single nucleotides, while indels may involve many base pairs. Although this might suggest that indels have a larger effect than base substitutions, single-base pair indels and gene-sized indels both result in gene disruption, thus generating more similar fitness effects regardless of the indel length. In fact, single base-pair indels in coding DNA may generate malformed gene products that require degradation, which might be even more harmful than entire gene deletions. Because the number of indel events, and not the size of indels, determines the genome-wide deleterious burden, we define the parameter u_{id} to be the number of indel mutation events per site per generation, and use this parameter to test the DBH.

MATERIALS AND METHODS

To examine the effect of genetic drift on mutation-rate evolution, it is necessary to derive accurate estimates of the mutation rate and genetic diversity across phylogenetically diverse organisms. Whole-genome sequencing (WGS) has greatly improved our ability to estimate such parameters. Highly accurate measurements of u_{bs} and u_{id} can be obtained through WGS of mutation-accumulation (MA) lines, in which repeated single-organism bottlenecks minimize the efficiency of selection, allowing for the accumulation of all but the most deleterious mutations (Lynch *et al.* 2008; Denver *et al.* 2009; Ossowski *et al.* 2010; Sung *et al.* 2012a, 2012b, 2015; Schrider *et al.* 2013). Along with data from prior MA studies, this study contains MA data from four new MA experiments. For new bacterial MA species, ~100 independent MA lines were initiated from a single founder colony. The new strains used were as follows: *Agrobacterium tumefaciens* str. C58, *Staphylococcus epidermidis* ATCC 12228, and *Vibrio cholerae* 2740-80.

Depending on the speed of growth, a single colony from each MA line was isolated and transferred to a fresh plate every 1–3 d over the course of the experiment. The bottlenecks process ensures that mutations accumulate in an effectively neutral fashion (Kibota and Lynch 1996). After each transfer, the original plate was retained as a backup plate at 4°. If the destination plate was contaminated, or if a single colony could not be picked, a single colony was transferred from the last 4° backup plate.

To estimate the generation times that occurred between each transfer, every 2 wk, an entire colony from five randomly selected MA lines was transferred to 1 × PBS saline buffer. These were vortexed, serially

diluted, and replated. Cell density was calculated from viable cell counts in both the growth conditions used throughout the bottleneck process as well as growth conditions at 4°. The total number of generations for each MA line was calculated by the average number of cell divisions per transfer multiplied by the total number of transfers. If backup plates were used, the average number of cell divisions at 4° was used in place of the average number of cell divisions per bottleneck at standard growth temperatures.

The average number of cell divisions across the MA are as follows (Dataset S1): *A. tumefaciens*, 5819; *Bacillus subtilis*, 5078 (Sung *et al.* 2015); *E. coli*, 4246 (Lee *et al.* 2012); *Mesoplasma florum*, 2351 (Sung *et al.* 2012a); *S. epidermidis*, 7170, and *V. cholerae*, 6453. The average number of generations used for reanalysis of the *C. elegans* MA study was 250 (Denver *et al.* 2009) (Dataset S2).

DNA extraction of MA lines was done using the wizard DNA extraction kit (Promega) or lysis media (CTAB or SDS) followed by phenol/chloroform extractions to Illumina library standards. Then, 101-bp paired-end Illumina (Illumina Hi-Seq platform) sequencing was applied to randomly selected MA lines of *A. tumefaciens*, *S. epidermidis*, and *V. cholerae*. Each MA line was sequenced to a coverage depth of ~100 ×, with an average library fragment size (distance between paired-end reads) of ~175 bp. The paired-end reads for each MA line were individually mapped against the reference genome (assembly and annotation available from the National Center for Biotechnology Information, <https://www.ncbi.nlm.nih.gov>) using two separate alignment algorithms: BWA v0.7.4 (Li and Durbin 2009) and NOVOALIGN v2.08.02 (available at www.novocraft.com). The resulting pileup files were converted to SAM format using SAMTOOLS v0.1.18 (Li *et al.* 2009). Using in-house perl scripts, the alignment information was further parsed to generate forward and reverse mapping information at each site, resulting in a configuration of eight numbers for each line (A, a, C, c, G, g, T, and t), corresponding to the number of reads mapped at each genomic position in the reference sequence. A separate file was also generated to display sites that had indel calls from the two alignment algorithms. Mutation calling was performed using a consensus method (Lynch *et al.* 2008; Denver *et al.* 2009; Ossowski *et al.* 2010; Lee *et al.* 2012; Sung *et al.* 2012a, 2012b, 2015).

A random subset of base-substitutions mutations called using these methods have been previously validated in *E. coli* and *B. subtilis* MA lines using fluorescent sequencing technology at the Indiana Molecular Biology Institute at Indiana University (Lee *et al.* 2012; Sung *et al.* 2015) (Dataset S3).

To verify indel mutations, we designed 38 primer sets to PCR amplify 300–500 bp regions surrounding the putative indel mutation in the *B. subtilis* MA lines (Dataset S4). All 29/29 short indels (< 10 bp) were directly confirmed using standard fluorescent sequencing technology. Two out of nine large indels (> 10 bp) were confirmed through sizing of the PCR product on gel electrophoresis. The remaining seven large indels did not amplify. For all cases, the indel was also confirmed to be absent in one other line without the mutation.

To calculate the base-substitution mutation rate per cell division for each line, we used the following equation:

$$u_{bs} = \frac{m}{nT},$$

where u_{bs} is the base-substitution mutation rate (per nucleotide site per generation), m is the number of observed base substitutions, n is the number of nucleotide sites analyzed, and T is the number of generations that occurred in the mutation-accumulation study. The SE for an individual line is calculated using (Denver *et al.* 2004, 2009):

$$SE_{\bar{x}} = \sqrt{\frac{u_{bs}}{nT}}.$$

The total SE of base-substitution mutation rate is given by the SD of the mutation rates across all lines (s) divided by the square root of the number of lines analyzed (N).

$$SE_{pooled} = \frac{s}{\sqrt{N}}$$

The same calculation was used to calculate indel mutation rate, with u_{bs} replaced with u_{id} .

Data availability

Illumina DNA sequences for the MA lines used in this study are deposited under the following Bioprojects: *A. tumefaciens* PRJNA256312, *B. subtilis* PRJNA256312, *M. florum* PRJNA256337, *S. epidermidis* PRJNA256338, and *V. cholerae* PRJNA256339.

File S1 contains detailed descriptions of eukaryotic u_{id} estimates, as well as calculations for G_e , G_{nc} , θ_s , π_s , and phylogenetic independent contrasts for both eukaryotic and prokaryotic organisms. Figure S1 contains average depth of sequencing coverage for each MA line in *A. tumefaciens*, *S. epidermidis*, and *V. cholerae*. Figure S2 displays the similarity in θ_s when increasing the number of unique alleles analyzed. Figure S3 shows the frequency distribution of mutant calls across MA lines. Table S1 contains the calculation for the estimated limit of selection to fix antimutators. Figure S4, Figure S5, Figure S6, and Table S2 contain statistical support for the DBH. Dataset S1, Dataset S2, Dataset S3, and Dataset S4 contain single nucleotide polymorphisms and indels for prokaryotic and eukaryotic organisms generated in this study.

RESULTS

To examine the effect of genetic drift on mutation-rate evolution, it is necessary to derive accurate estimates of the mutation rate and genetic diversity across phylogenetically diverse organisms. WGS has greatly improved our ability to estimate such parameters. Highly accurate measurements of u_{bs} and u_{id} can be obtained through WGS of MA lines, in which repeated single-organism bottlenecks minimize the efficiency of selection, allowing for the accumulation of all but the most deleterious mutations (Lynch *et al.* 2008; Denver *et al.* 2009; Ossowski *et al.* 2010; Sung *et al.* 2012a, 2012b, 2015; Schrider *et al.* 2013).

The power of genetic drift is related to the inverse of the effective population size [$1/N_e$ for haploids, $1/(2N_e)$ for diploids]. Under the assumption of neutrality, the effective population size (N_e) can be estimated from the average nucleotide heterozygosity at silent sites in natural populations (π_s), or as a function of the number of segregating sites in the population (θ_s), both of which lead to expected values equal to $4N_e u_{bs}$ in diploids and $2N_e u_{bs}$ in haploids (Kimura 1983). For most organisms analyzed in this study, enough WGS data were available to allow calculation of species-specific θ_s values (see File S1 and Table 1). For the remaining species, we pooled large available multilocus-sequence studies to estimate π_s . In all cases, we set the estimates of θ_s or π_s equal to $4N_e u_{bs}$ in diploids ($2N_e u_{bs}$ in haploids), and solved for N_e by factoring out u_{bs} . Because this calculation only involves u_{bs} , the estimate of N_e is uninfluenced by sampling error in u_{id} , thus providing an independent trait measurement by which to test the DBH (see File S1 for further evaluation of the nonindependence issue).

To provide additional data for testing whether the power of genetic drift constrains the lower limit of indel mutation-rate evolution, we performed MA experiments in *A. tumefaciens* str. C58, *S. epidermidis* ATCC 12228, and *V. cholerae* 2740-80. Each bacterial MA experiment was initiated from multiple lines derived from a single progenitor

Table 1 Effective genome size (G_e), indel events per site per generation (u_{id}), base-substitution mutation rate per generation (u_{bs}), θ_s (or π_s , denoted by *) measurements for population mutation rate (Watterson 1975; Tajima 1989; Fu 1995), and estimated effective population size (N_e) for seven prokaryotic and eight eukaryotic organisms (see File S1 for details)

Species	Label	G_e ($\times 10^7$ Sites)	$G_c + G_{nc}$ ($\times 10^7$ Sites)	u_{id} ($\times 10^{-10}$ per Site per Generation)	u_{bs} ($\times 10^{-10}$ Events per Site per Generation)	θ_s or π_s	N_e ($\times 10^6$)
Prokaryotes							
<i>Agrobacterium tumefaciens</i>	Agt	0.50	0.57	0.30	2.92	0.200*	342.47
<i>Bacillus subtilis</i>	Bs	0.36	0.43	1.20 ^d	3.35 ^d	0.041	61.19
<i>Escherichia coli</i>	Ec	0.39	0.46	0.37 ^e	2.00 ^e	0.071	179.60
<i>Mesoplasma florum</i>	Mf	0.07	0.08	23.10 ^f	97.80 ^f	0.021	1.07
<i>Pseudomonas aeruginosa</i>	Pa	0.59	0.67	0.14 ^g	0.79 ^g	0.033*	210.70
<i>Staphylococcus epidermidis</i>	Se	0.21	0.26	1.13	7.40	0.052	35.14
<i>Vibrio cholerae</i>	Vc	0.34	0.39	0.18	1.15	0.110	478.26
Eukaryotes							
<i>Arabidopsis thaliana</i>	At	4.21	5.55 ^a	11.20 ^h	69.50 ^{h,p}	0.008	0.29
<i>Caenorhabditis elegans</i>	Ce	2.50	6.37 ^b	6.69 ⁱ	14.50 ^q	0.003	0.54
<i>Chlamydomonas reinhardtii</i>	Cr	3.92	5.51	0.44 ^j	3.80 ^j	0.032	43.31
<i>Drosophila melanogaster</i>	Dm	2.32	8.86 ^c	4.61 ^k	51.65 ^k	0.018	0.86
<i>Homo sapiens</i>	Hs	3.65	21.75 ^b	18.20 ^l	135.13 ^l	0.001	0.02
<i>Mus musculus</i>	Mm	3.55	27.17 ^b	3.10 ^m	54.00 ^m	0.004*	1.77
<i>Paramecium tetraurelia</i>	Pt	5.68	7.28	0.04 ⁿ	0.19 ⁿ	0.008	101.80
<i>Saccharomyces cerevisiae</i>	Sc	0.87	1.02 ^b	0.92 ^o	2.63 ^o	0.004	7.78

$G_c + G_{nc}$ is the effective genome size when including the total amount of coding (G_c) and noncoding DNA (G_{nc}) that is estimated to be under purifying selection. Footnotes in u_{id} and u_{bs} indicate data sources (rates pooled when multiple data sources are available), and, when absent, indicate data generated in this study (see

Materials and Methods).

^aHaudry et al. (2013).

^bSiepel et al. (2005).

^cHalligan et al. (2004).

^dSung et al. (2015).

^eLee et al. (2012).

^fSung et al. (2012a).

^gSung et al. (2012b).

^hOssowski et al. (2010).

ⁱLipinski et al. (2011).

^jSung et al. (2012a); Ness et al. (2015).

^kSchrider et al. (2013).

^lConrad et al. (2011); O'Roak et al. (2011, 2012); Kong et al. (2012); Campbell and Eichler (2013); Wang and Zhu (2014); The 1000 Genomes Project Consortium (2015).

^mUchimura et al. (2015).

ⁿSung et al. (2012b).

^oLynch et al. 2008; (Zhu et al. 2014).

^pOssowski et al. (2010); (Yang et al. 2015).

^qLipinski et al. (2011).

colony, each of which was repeatedly bottlenecked to accumulate mutations for an average of 5819, 7170, and 6453 generations, respectively (see Materials and Methods; harmonic mean population sizes between transfers were 13.4 (0.1), 12.6 (0.3), and 14.9 (0.2), respectively). Then, 101-bp paired-end WGS was applied to randomly selected MA lines (47 *A. tumefaciens*, 22 *S. epidermidis*, and 46 *V. cholerae* MA lines, Dataset S1). The average sequencing coverage depth is greater than $20 \times$ per site across all MA lines surveyed in these organisms (Figure S1), and greater than $50 \times$ per site for 93.75% (150/160) of the MA lines, providing high accuracy for measurement of u_{bs} and u_{id} . Mutations were called and categorized for each of the three species (Dataset S3 and Dataset S4), with u_{bs} and u_{id} shown in Table 1.

To test the DBH, we combined u_{bs} and u_{id} from the three bacterial species analyzed in this study with u_{bs} and u_{id} from four bacterial and eight eukaryotic MA WGS studies (Table 1, Dataset S1, Dataset S2, Dataset S3, and Dataset S4), and also included the same estimates for human derived from WGS of parent-offspring trios. u_{id} includes all indel events in each of the 15 study species (see File S1). Due to the highly repetitive DNA sequence in eukaryotic genomes, the number of large indels events (> 9 bp) in eukaryotes may be downwardly biased when using WGS methods. Therefore, our es-

timate of the number of large indel events also includes events identified by comparative genome hybridization arrays for organisms where data were available (Lynch et al. 2008; Lipinski et al. 2011). Large indel events only account for 15.0% of total indels events across the study bacteria (76/506, Dataset S4), suggesting that any underestimation of the number of large indel events should only have a small effect on u_{id} .

To determine the genome-wide deleterious burden in each organism associated with indel mutations, we multiplied u_{id} with G_e , approximating the latter by the proteome size of that organism. A plot of the logs of the two parameters of $u_{id}G_e$ and N_e against one another yields a strong negative correlation across all of cellular life (Figure 1A, $r^2 = 0.89$). Because the power of genetic drift is inversely proportional to N_e , this observation is consistent with the idea that selection operates to reduce mutation rates to a barrier imposed by random genetic drift. Phylogenetic nonindependence may complicate observed relationships between genomic attributes and N_e (Whitney and Garland 2010). However, the relationship between N_e and $u_{id}G_e$ remains robust even after phylogenetic correction (Figure 2, A and B, $r^2 = 0.83$), indicating that the correlation between N_e and $u_{id}G_e$ reflects a true biological phenomenon across the Tree of Life.

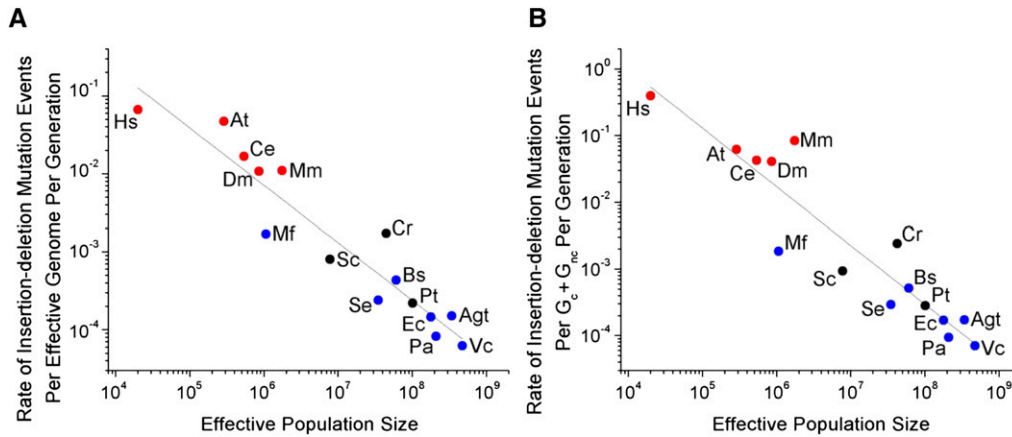


Figure 1 Relationship between the rate of indel events per generation per effective genome ($u_{id}G_e$) and effective population size (N_e). (A) Regression: $\log_{10}(u_{id}G_e) = 2.23(0.48) - 0.73(0.07)\log_{10}N_e$ ($r^2 = 0.89$, $P = 6.81 \times 10^{-8}$, d.f. = 13), with SE of parameter estimates shown in parentheses. Blue circles represent bacteria, red circles multicellular eukaryotes, and black circles unicellular eukaryotes, with all data summarized in Table 1. The full list of indel events for analyzed organisms is presented in Dataset S4.

Chromosomal distributions of indel events at each site across all mutation-accumulation experiments are shown in Figure S1, A and B. (B) Relationship when adding the number of estimated noncoding sites under purifying selection to the effective genome size ($G_c + G_{nc}$) for eukaryotic organisms. Regression: $\log_{10}[u_{id}(G_c + G_{nc})] = 3.49(0.66) - 0.87(0.09)\log_{10}N_e$ ($r^2 = 0.87$, $P = 3.13 \times 10^{-7}$, d.f. = 13).

DISCUSSION

Because the DBH makes general predictions about the pattern of molecular and cellular evolution across the Tree of Life, because our focus is on one of the central determining factors in the evolutionary process (the mutation rate), and because the patterns appear so strong, it is essential to consider the range of factors that might give rise to the observed statistical relationships, and also to alternative evolutionary hypotheses for them. We first consider three issues with respect to estimating the key parameters N_e , u_{bs} , u_{id} , and G_e and then elaborate on the significance and implications of the relationship between $u_{id}G_e$ and N_e for our understanding of molecular evolution.

First, we address the estimation of N_e , one of the most difficult issues in empirical population genetics. Because populations fluctuate in density over time, any estimate of N_e must reflect a long-term average, presumably approximating a harmonic mean, not the immediate population state. Because evolution is a long-term process, however, the mean is most relevant to the issues being examined herein. Recent selective sweeps or population bottlenecks can transiently modify levels of genetic variation at individual loci (Charlesworth 2009; Karasov *et al.* 2010), introducing noise into any estimates of N_e derived from limited numbers of genetic loci, but this would reduce the strength of any true underlying correlation between the rate of mutation ($u_{id}G_e$), and long-term N_e , *i.e.*, would operate against our ability to detect the expected signal of the DBH.

Such effects are especially likely in asexual species, where the possibility of reduced recombination might subject many neutral nucleotide sites to the effects of selection on nearby, linked sites. Thus, to minimize sampling error, wherever possible, we have relied upon genome-wide sampling of the number of segregating sites to obtain a low-variance estimator of $N_e u$ from observations on silent sites (Watterson 1975). The utilization of an average θ_s across a large number of nucleotide sites and individual isolates reduces the effects of evolutionary sampling variance associated with chromosomally localized and population-specific sweeps arising within individual species (Fu and Li 1993). Using available genomic data, we calculated θ_s across a large number of within-species genotypic isolates, excluding nearly identical lab strains that originated from the same individual (see *Materials and Methods*). Although no estimates of silent-site diversity (the source of N_e estimates) are without error, estimates derived from segregating polymorphic sites across large-scale genomic data sets appear quite robust (Figure S2). Moreover, should the levels of variation

sampled in our various study species reflect recent events, to which mutation-rate evolution has not had adequate time to respond (Brandvain and Wright 2016), this would only introduce noise into the relationship between effective population size and mutation rates.

Second, as we have noted earlier, there is some concern that correlations between estimates of mutation rates and N_e could, in part, be spurious artifacts resulting from the use of estimates of N_e obtained by dividing measures of standing variation at silent-sites by u_{bs} (Sung *et al.* 2012a). If the sampling variance of u_{bs} is substantial enough, this could lead to a negative correlation between the observed u_{bs} and extrapolated N_e estimates, and, if there were a sampling covariance between u_{bs} and u_{id} , this could carry over into the current study. In the Supplemental Material (File S1, Figure S4, Figure S5, Figure S6 and Figure S7), we provide complementary analyses to that in Sung *et al.* (2012a), indicating that the sampling variance of u_{bs} from WGS-MA studies is not large enough to explain the negative correlation previously seen between u_{bs} and N_e estimates. Because u_{bs} and u_{id} are measured by different methods, the sampling covariance between these two measures is expected to be negligible. We emphasize that it is the sampling variance, not the evolutionary variance, that is of concern here. The variance of the log-scaled values of u_{bs} would have to exceed the log-scaled values of N_e by \sim two orders of magnitude in order to create the negative correlations that we observe (File S1). As an extreme way of looking at the situation, if silent-site variation were constant across all taxa, and the parametric values of mutation rates and N_e were obtained without error, the only explanation for the data would be a true underlying negative evolutionary covariance between the two features. In fact, there is a marginal negative correlation between estimates of π_s and u_{bs} (Figure S3, Figure S4, Figure S5, Figure S6, Figure S7, and Table S2), further bolstering the idea that u_{bs} and u_{id} decline evolutionarily as N_e increases.

Third, the DBH proposes that the strength of selection operating to reduce the indel mutation rate is based upon the total indel deleterious mutational load, *i.e.*, the product of the mutational rate of appearance of indels at individual nucleotide sites (u_{id}), and the number of sites under selective constraint in the genome (G_e , approximated by the proteome size of the organism). However, some noncoding DNA (*e.g.*, noncoding functional RNAs, and *cis*-regulatory units in untranslated regions or introns) is certainly under selective constraint, with mutations at these sites increasing the deleterious mutational load. Thus, it can be argued that the estimated number of nucleotides affecting fitness (G_e) scales

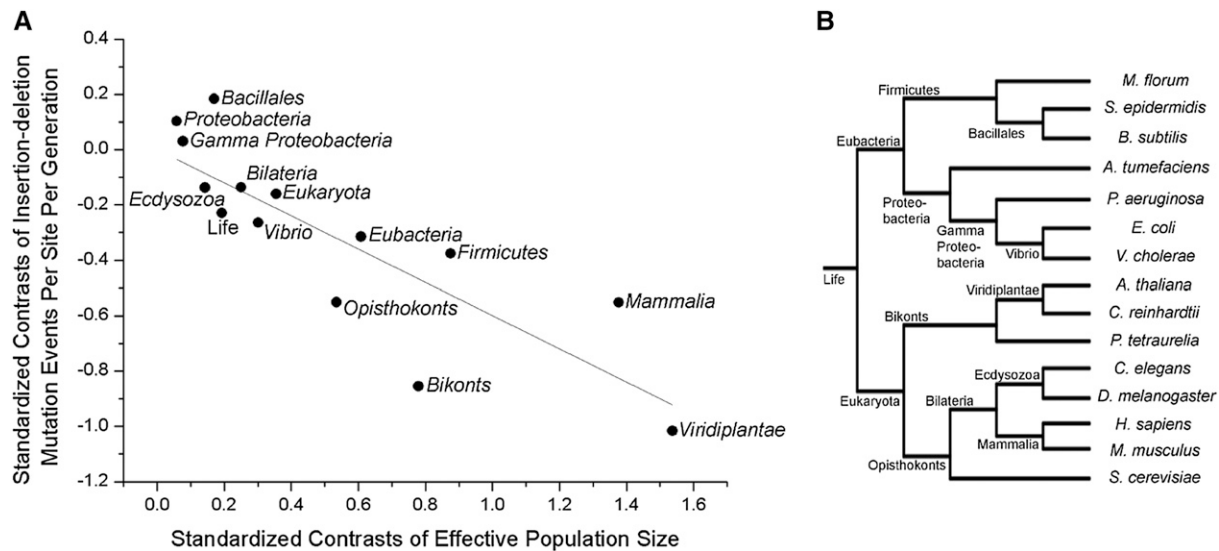


Figure 2 Relationship between indel events per site per generation ($u_{id}G_e$) and effective population size (N_e) after phylogenetic correction. (A) Standardized phylogenetically independent contrasts performed using Compare (Martins 2004), and the PDAP module in Mesquite (Garland *et al.* 1993), with branch lengths of 1.0. The regression equation of the contrasts through the origin is: $u_{id}G_e = -0.60(0.07)N_e$ ($r^2 = 0.83$, $P = 1.28 \times 10^{-6}$, d.f. = 13), with SE in parentheses. (B) Phylogenetic tree showing the relationship between organisms.

differently than the protein-coding region of the genome, particularly in larger eukaryotic genomes with a considerable number of noncoding sites (Halligan *et al.* 2004; Siepel *et al.* 2005; Halligan and Keightley 2006). Difficulties can arise when estimating the proportion of noncoding DNA that is under selective constraint (G_{nc}), as the estimated number of such sites can vary greatly depending on the model used to define noncoding DNA, and the identification of conserved noncoding DNA is highly sensitive to the available phylogeny (Siepel *et al.* 2005). Nevertheless, if we sum the estimated total amount of noncoding DNA under selective constraint (G_{nc} , see File S1) with that of coding DNA (G_c), we find that $u_{id}(G_c + G_{nc})$ and N_e remain highly correlated (Figure 1B, $r^2 = 0.87$), simply because the fraction of functional noncoding DNA increases with the total amount of coding DNA.

We currently adhere to the DBH as an explanation for the phylogenetic pattern of mutation-rate variation primarily because it has been difficult to reconcile the patterns with alternative hypotheses. In the introduction, we provided arguments as to why selection for replication speed appears to be unlikely to explain a negative correlation between mutation rates and population size in unicellular species, and, in multicellular species, the simultaneous deployment of hundreds to thousands of origins of replication makes such an explanation even more unlikely. Nor does a general constraint on replication fidelity explain the data.

A second potential explanation for variation in the per-generation mutation rate is that it is driven largely by variation in numbers of germline cell divisions (Ness *et al.* 2012), but this cannot be reconciled with the fact that the base-substitution mutation rate scales negatively with N_e in analyses entirely restricted to unicellular species (Sung *et al.* 2012a). In all such species, there is one cell division per generation, and yet the base-substitution mutation rate per site per cell division ranges from $\sim 10^{-11}$ in *Paramecium tetraurelia* (Sung *et al.* 2012b) to $\sim 10^{-8}$ in *M. florum* (Sung *et al.* 2012a). Similarly, the number of indel mutational events per site per cell division differs by over two orders of magnitude across unicellular organisms (Table 1 and Figure 3), and the negative regression with N_e remains significant when confined to unicellular species (Figure 1, $r^2 = 0.66$, $P = 0.003$).

A third hypothesis for mutation-rate evolution is that selection is effective enough to reduce the error rate to the point at which the physical laws of thermodynamics take over (Kimura 1967). However, it is difficult to reconcile this argument with the data now showing that mutation rates vary by three orders of magnitude, as there are no known mechanisms by which basic biophysical features (such as diffusion coefficients and stochastic molecular motion) would vary by this degree among the cytoplasm of different taxa. There is, of course, the issue of evolved differences in the biochemical features and efficiency of operation of the proteins involved in replication and repair. However, this type of variation is in the explanatory domain of the DBH. The DBH postulates that replication fidelity is typically not at the maximum possible level of refinement, but just the lowest level possible under the prevailing level of random genetic drift, which varies substantially among lineages.

That a decline in replication fidelity should decline with decreasing effective population size appears to be a unique prediction of the DBH. Although other theoretical work has been done on mutation-rate evolution, in no case is this type of scaling obviously predicted (acknowledging that this has not been a central focus of such work). For example, allowing for a role of beneficial mutations, Kimura (1967) and Leigh (1970) suggested that the long-term rate of adaptation is maximized when the genome-wide mutation rate equals the rate of population fixation of beneficial mutations. The precise predictions of this hypothesis are not entirely clear, but because mutations arise at a higher rate in large populations, and, if beneficial, fix with higher probabilities, a positive association between the mutation rate and N_e seems to be implied. A rather different model argues that populations should evolve genome-wide mutation rates equal to the average effect of a deleterious mutation (Orr 2000; Johnson and Barton 2002), which seems to imply an optimal mutation rate independent of population size (unless one wishes to postulate an association between average mutational effect and N_e , for which we are unaware of any evidence).

The DBH proposes that new alleles that reduce the genome-wide indel mutation rate (*i.e.*, anti-mutators) can be promoted by selection only if they provide a significant enough advantage to offset the power

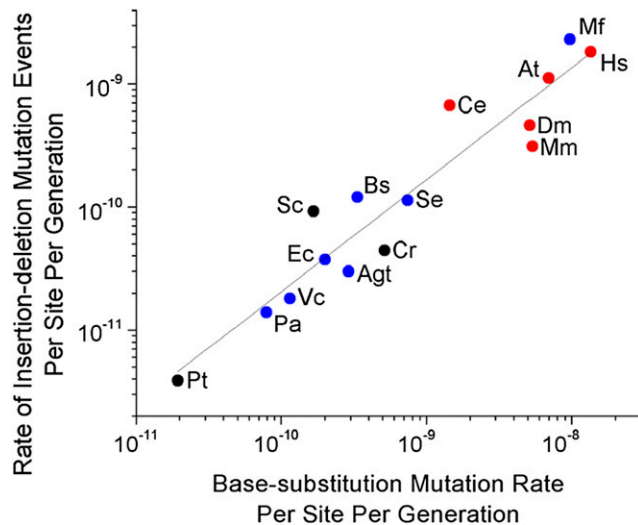


Figure 3 Relationship between the rate of indel events per site per generation (u_{id}), and the base-substitution mutation rate per site per generation (u_{bs}). Regression: $\log_{10}(u_{id}) = -1.56(0.74) + 0.91(0.08)\log_{10}u_{bs}$ ($r^2 = 0.90$, $P = 4.13 \times 10^{-8}$, d.f. = 13). SE measurements are shown in parentheses. Blue circles represent eubacteria, red circles multicellular eukaryotes, and black circles unicellular eukaryotes, with all data summarized in Table 1.

of genetic drift. The average selective effect of an antimutator or mutator allele (which operate opposite to each other) can be approximated by $st\Delta U_{id}$, with ΔU_{id} representing the change in the genome-wide indel mutation rate with respect to the population mean rate, s being the average reduction in fitness per mutation (Lynch 2010), and t being the number of generations a mutation remains associated with its mutator genetic background (Lynch 2011). ΔU_{id} can be approximated by the change in the indel mutation rate over the effective genome, or $\Delta u_{id}G_e$ (Lynch 2011). By setting $st\Delta u_{id}G_e$ equal to the power of random genetic drift [$1/N_e$ for haploids, $1/(2N_e)$ for diploids], we can acquire some sense of the average reduction in the indel mutation rate that is required for the power of selection to exceed power of genetic drift. Using estimates of an average value of the selective coefficient ($s = 0.01$) (Lynch *et al.* 1999; Eyre-Walker and Keightley 2007), and assuming that free recombination unlinks mutation-rate modifier alleles from their background every ~ 2 generations in sexually outcrossing species ($t = 2$) (Lynch 2010), solving $st\Delta u_{id}G_e = 1/N_e$ [= $1/(2N_e)$ for diploids] for Δu_{id} suggests that the average antimutator must reduce the indel mutation rate by greater than ~ 0.1 – 1% in most organisms (Table S1) in order to be promoted by selection. One major limitation of this kind of analysis is that values of s and t are not well known, and are likely vary across organisms. A second and equally important caveat is that the prior analysis assumes that mutator and antimutator alleles arise with equal frequency. Owing to the high level of refinement of the replication and repair machinery, it seems much more likely that mutations involving the components of such machinery will increase rather than decrease the mutation rate. This will push the equilibrium mutation rate to higher levels than expected (Lynch 2008), although without quantitative information on such bias, it is difficult to determine the exact position at which the mutation rate will stall.

Finally, we note that because recombination unlinks alleles from their genetic background, the capacity of selection to enhance replication fidelity is ultimately a function of the recombination rate (Kimura 1967; Lynch 2008). Thus, it may be viewed as surprising that bacteria, which do not undergo meiotic recombination, exhibit a relationship between

u_{id} and N_e similar to that in eukaryotic species engaging in periodic to regular meiosis (Figure 1, A and B). It should be noted, however, that bacterial recombination occurs through multiple mechanisms (transformation, conjugation, and/or transduction). Many bacterial species are known to naturally undergo high rates of recombination, with ratios of recombination to mutation rates frequently being comparable to those in multicellular eukaryotes (Feil and Spratt 2001; Lynch 2007; Doroghazi *et al.* 2014; Lassalle *et al.* 2015), so, in this sense, comparable behavior of bacterial and eukaryotic species is not unexpected.

In summary, as in our previous work on the base-substitution mutation rate (Sung *et al.* 2012a), the strong correlation between the genome-wide indel rate and N_e appears not to be a statistical artifact. Moreover, among various hypotheses that have been suggested for mutation-rate evolution, the DBH appears to provide the most compatible explanation for the ~ 1000 -fold range of variation of this trait across the Tree of Life. As noted above, the molecular mechanisms that generate and resolve base-substitution and indel mutations differ in a number of ways, and the rate of occurrence of these two types of mutations differ by one to two orders of magnitude (with u_{id} ranging from 1.8 to 11.9% of u_{bs} , presumably because of the elevated deleterious effects of indel mutations). Yet, despite these differences, both u_{bs} and u_{id} scale similarly with changes in N_e (Figure 3, $r^2 = 0.89$). Because the forces of mutation, selection, and drift apply to all biological traits, the maximum achievable level of refinement for other fundamental cellular traits may also be influenced by the drift barrier.

ACKNOWLEDGMENTS

Support was provided by the Multidisciplinary University Research Initiative Award W911NF-09-1-0444, and from the US Army Research Office to M. L., P. Foster, H. Tang, and S. Finkel, and W911NF-14-1-0411 to M. L., P. Foster, J. McKinlay, and J. T. Lennon, by CAREER award DEB-0845851 from the National Science Foundation to V. C., and by National Institutes of Health Awards F32-GM103164 to W.S., and R01-GM036827 to M. L. and W. K. Thomas. This material is based upon work supported by the National Science Foundation under grant no. CNS-0521433, CNS-0723054, and ABI-1062432 to Indiana University.

Author contributions: W.S., C.F., V.C., and M.L. designed the research; W.S., M.A., M.D., and T.P. performed the research; W.S. and M.A. analyzed the data; and W.S., M.A., and M.L. wrote the paper.

LITERATURE CITED

- Brandvain, Y., and S. I. Wright, 2016 The limits of natural selection in a nonequilibrium world. *Trends Genet.* 32: 201–210.
- Campbell, C. D., and E. E. Eichler, 2013 Properties and rates of germline mutations in humans. *Trends Genet.* 29: 575–584.
- Charlesworth, B., 2009 Fundamental concepts in genetics: effective population size and patterns of molecular evolution and variation. *Nat. Rev. Genet.* 10: 195–205.
- Conrad, D. F., J. E. Keebler, M. A. DePristo, S. J. Lindsay, Y. Zhang *et al.*, 2011 Variation in genome-wide mutation rates within and between human families. *Nat. Genet.* 43: 712–714.
- Denver, D. R., K. Morris, M. Lynch, and W. K. Thomas, 2004 High mutation rate and predominance of insertions in the *Caenorhabditis elegans* nuclear genome. *Nature* 430: 679–682.
- Denver, D. R., S. Feinberg, S. Estes, W. K. Thomas, and M. Lynch, 2005 Mutation rates, spectra and hotspots in mismatch repair-deficient *Caenorhabditis elegans*. *Genetics* 170: 107–113.
- Denver, D. R., P. C. Dolan, L. J. Wilhelm, W. Sung, J. I. Lucas-Lledo *et al.*, 2009 A genome-wide view of *Caenorhabditis elegans* base-substitution mutation processes. *Proc. Natl. Acad. Sci. USA* 106: 16310–16314.

- Doroghazi, J. R., and D. H. Buckley, 2014 Intraspecies comparison of *Streptomyces pratensis* genomes reveals high levels of recombination and gene conservation between strains of disparate geographic origin. *BMC Genomics* 15: 970.
- Drake, J. W., 1991 A constant rate of spontaneous mutation in DNA-based microbes. *Proc. Natl. Acad. Sci. USA* 88: 7160–7164.
- Drake, J. W., B. Charlesworth, D. Charlesworth, and J. F. Crow, 1998 Rates of spontaneous mutation. *Genetics* 148: 1667–1686.
- Eyre-Walker, A., and P. D. Keightley, 2007 The distribution of fitness effects of new mutations. *Nat. Rev. Genet.* 8: 610–618.
- Feil, E. J., and B. G. Spratt, 2011 Recombination and the population structures of bacterial pathogens. *Annu. Rev. Microbiol.* 55: 561–590.
- Fu, Y. X., 1995 Statistical properties of segregating sites. *Theor. Popul. Biol.* 48: 172–197.
- Fu, Y. X., and W. H. Li, 1993 Statistical tests of neutrality of mutations. *Genetics* 133: 693–709.
- Garland, T., A. W. Dickerman, C. M. Janis, and J. A. Jones, 1993 Phylogenetic analysis of covariance by computer-simulation. *Syst. Biol.* 42: 265–292.
- Halligan, D. L., and P. D. Keightley, 2006 Ubiquitous selective constraints in the *Drosophila* genome revealed by a genome-wide interspecies comparison. *Genome Res.* 16: 875–884.
- Halligan, D. L., A. Eyre-Walker, P. Andolfatto, and P. D. Keightley, 2004 Patterns of evolutionary constraints in intronic and intergenic DNA of *Drosophila*. *Genome Res.* 14: 273–279.
- Haudry, A., A. E. Platts, E. Vello, D. R. Hoen, M. Leclercq *et al.*, 2013 An atlas of over 90,000 conserved noncoding sequences provides insight into crucifer regulatory regions. *Nat. Genet.* 45: 891–898.
- Johnson, T., and N. H. Barton, 2002 The effect of deleterious alleles on adaptation in asexual populations. *Genetics* 162: 395–411.
- Karason, T., P. W. Messer, and D. A. Petrov, 2010 Evidence that adaptation in *Drosophila* is not limited by mutation at single sites. *PLoS Genet.* 6: e1000924.
- Kibota, T. T., and M. Lynch, 1996 Estimate of the genomic mutation rate deleterious to overall fitness in *E. coli*. *Nature* 381: 694–696.
- Kimura, M., 1967 On the evolutionary adjustment of spontaneous mutation rates. *Genet. Res.* 9: 23–24.
- Kimura, M., 1983 *The Neutral Theory of Molecular Evolution*, Cambridge University Press, Cambridge, UK.
- Kong, A., M. L. Frigge, G. Masson, S. Besenbacher, P. Sulem *et al.*, 2012 Rate of *de novo* mutations and the importance of father's age to disease risk. *Nature* 488: 471–475.
- Krokan, H. E., and M. Bjoras, 2013 Base excision repair. *Cold Spring Harb. Perspect. Biol.* 5: a012583.
- Kunkel, T. A., 2009 Evolving views of DNA replication (in)fidelity. *Cold Spring Harb. Symp. Quant. Biol.* 74: 91–101.
- Lassalle, F., S. Perian, T. Bataillon, X. Nesme, L. Duret *et al.*, 2015 GC-Content evolution in bacterial genomes: the biased gene conversion hypothesis expands. *PLoS Genet.* 11: e1004941.
- Lee, H., E. Popodi, H. Tang, and P. L. Foster, 2012 Rate and molecular spectrum of spontaneous mutations in the bacterium *Escherichia coli* as determined by whole-genome sequencing. *Proc. Natl. Acad. Sci. USA* 109: e2774–e2783.
- Leigh, E. G., Jr., 1970 Natural selection and mutability. *Am. Nat.* 104: 301–305.
- Li, H., and R. Durbin, 2009 Fast and accurate short read alignment with Burrows-Wheeler transform. *Bioinformatics* 25: 1754–1760.
- Li, H., B. Handsaker, A. Wysoker, T. Fennell, J. Ruan *et al.*, 2009 The sequence alignment/map format and SAMtools. *Bioinformatics* 25: 2078–2079.
- Lipinski, K. J., J. C. Farslow, K. A. Fitzpatrick, M. Lynch, V. Katju *et al.*, 2011 High spontaneous rate of gene duplication in *Caenorhabditis elegans*. *Curr. Biol.* 21: 306–310.
- Loh, E., J. J. Salk, and L. A. Loeb, 2010 Optimization of DNA polymerase mutation rates during bacterial evolution. *Proc. Natl. Acad. Sci. USA* 107: 1154–1159.
- Lynch, M., 2007 *The Origins of Genome Architecture*, Sinauer Associates, Sunderland, Massachusetts.
- Lynch, M., 2008 The cellular, developmental and population-genetic determinants of mutation-rate evolution. *Genetics* 180: 933–943.
- Lynch, M., 2010 Evolution of the mutation rate. *Trends Genet.* 26: 345–352.
- Lynch, M., 2011 The lower bound to the evolution of mutation rates. *Genome Biol. Evol.* 3: 1107–1118.
- Lynch, M., and G. K. Marinov, 2015 The bioenergetic costs of a gene. *Proc. Natl. Acad. Sci. USA* 112: 15690–15695.
- Lynch, M., J. Blanchard, D. Houle, T. Kibota, S. Schultz *et al.*, 1999 Spontaneous deleterious mutation. *Evolution* 53: 645–663.
- Lynch, M., W. Sung, K. Morris, N. Coffey, C. R. Landry *et al.*, 2008 A genome-wide view of the spectrum of spontaneous mutations in yeast. *Proc. Natl. Acad. Sci. USA* 105: 9272–9277.
- Martins, E. P., 2004 *Compare, Version 4.6b. Computer Programs for the Statistical Analysis of Comparative Data*. Department of Biology, Indiana University, Bloomington, IN. Available at: <http://compare.bio.indiana.edu>.
- McCulloch, S. D., and T. A. Kunkel, 2008 The fidelity of DNA synthesis by eukaryotic replicative and translesion synthesis polymerases. *Cell Res.* 18: 148–161.
- Mira, A., H. Ochman, and N. A. Moran, 2001 Deletional bias and the evolution of bacterial genomes. *Trends Genet.* 17: 589–596.
- Morita, R., S. Nakane, A. Shimada, M. Inoue, H. Iino *et al.*, 2010 Molecular mechanisms of the whole DNA repair system: a comparison of bacterial and eukaryotic systems. *J. Nucleic Acids* 2010: 179594.
- Ness, R. W., A. D. Morgan, N. Colegrave, and P. D. Keightley, 2012 Estimate of the spontaneous mutation rate in *Chlamydomonas reinhardtii*. *Genetics* 192: 1447–1454.
- Ness, R. W., S. A. Kraemer, N. Colegrave, and P. D. Keightley, 2015 Direct estimate of the spontaneous mutation rate uncovers the effects of drift and recombination in the *Chlamydomonas reinhardtii* plastid genome. *Mol. Biol. Evol.* 33: 800–808.
- O’Roak, B. J., P. Deriziotis, C. Lee, L. Vives, J. J. Schwartz *et al.*, 2011 Exome sequencing in sporadic autism spectrum disorders identifies severe *de novo* mutations. *Nat. Genet.* 43: 585–589.
- O’Roak, B. J., L. Vives, S. Girirajan, E. Karakoc, N. Krumm *et al.*, 2012 Sporadic autism exomes reveal a highly interconnected protein network of *de novo* mutations. *Nature* 485: 246–250.
- Orr, H. A., 2000 The rate of adaptation in asexuals. *Genetics* 155: 961–968.
- Ossowski, S., K. Schneeberger, J. I. Lucas-Lledo, N. Warthmann, R. M. Clark *et al.*, 2010 The rate and molecular spectrum of spontaneous mutations in *Arabidopsis thaliana*. *Science* 327: 92–94.
- Sancar, A., L. A. Lindsey-Boltz, K. Unsal-Kacmaz, and S. Linn, 2004 Molecular mechanisms of mammalian DNA repair and the DNA damage checkpoints. *Annu. Rev. Biochem.* 73: 39–85.
- Schrider, D. R., D. Houle, M. Lynch, and M. W. Hahn, 2013 Rates and genomic consequences of spontaneous mutational events in *Drosophila melanogaster*. *Genetics* 194: 937–954.
- Siepel, A., G. Bejerano, J. S. Pedersen, A. S. Hinrichs, M. Hou *et al.*, 2005 Evolutionarily conserved elements in vertebrate, insect, worm, and yeast genomes. *Genome Res.* 15: 1034–1050.
- Sniegowski, P., and Y. Raynes, 2013 Mutation rates: how low can you go? *Curr. Biol.* 23: R147–R149.
- Sniegowski, P. D., P. J. Gerrish, T. Johnson, and A. Shaver, 2000 The evolution of mutation rates: separating causes from consequences. *BioEssays* 22: 1057–1066.
- Sung, W., M. S. Ackerman, S. F. Miller, T. G. Doak, and M. Lynch, 2012a Drift-barrier hypothesis and mutation-rate evolution. *Proc. Natl. Acad. Sci. USA* 109: 18488–18492.
- Sung, W., A. E. Tucker, T. G. Doak, E. Choi, W. K. Thomas *et al.*, 2012b Extraordinary genome stability in the ciliate *Paramecium tetraurelia*. *Proc. Natl. Acad. Sci. USA* 109: 19339–19344.
- Sung, W., M. S. Ackerman, J. F. Gout, S. F. Miller, E. Williams *et al.*, 2015 Asymmetric context-dependent mutation patterns revealed through mutation-accumulation experiments. *Mol. Biol. Evol.* 32: 1672–1683.

- Tajima, F., 1989 Statistical method for testing the neutral mutation hypothesis by DNA polymorphism. *Genetics* 123: 585–595.
- The 1000 Genomes Project Consortium, 2015 A global reference for human genetic variation. *Nature* 526: 68–74.
- Uchimura, A., M. Higuchi, Y. Minakuchi, M. Ohno, A. Toyoda *et al.*, 2015 Germline mutation rates and the long-term phenotypic effects of mutation accumulation in wild-type laboratory mice and mutator mice. *Genome Res.* 25: 1125–1134.
- Vieira-Silva, S., M. Touchon, and E. P. Rocha, 2010 No evidence for elemental-based streamlining of prokaryotic genomes. *Trends Ecol. Evol.* 25: 319–320; author reply 320–311.
- Wang, H., and X. Zhu, 2014 *De novo* mutations discovered in 8 Mexican American families through whole genome sequencing. *BMC Proc.* 8: S24.
- Watterson, G. A., 1975 On the number of segregating sites in genetical models without recombination. *Theor. Popul. Biol.* 7: 256–276.
- Whitney, K. D., and T. Garland, Jr., 2010 Did genetic drift drive increases in genome complexity? *PLoS Genet.* 6: e1001080.
- Yang, S., L. Wang, J. Huang, X. Zhang, Y. Yuan *et al.*, 2015 Parent-progeny sequencing indicates higher mutation rates in heterozygotes. *Nature* 523: 463–467.
- Zhu, Y. O., M. L. Siegal, D. W. Hall, and D. A. Petrov, 2014 Precise estimates of mutation rate and spectrum in yeast. *Proc. Natl. Acad. Sci. USA* 111: e2310–e2318.

Communicating editor: S. I. Wright